Am J Cancer Res 2020;10(11):3752-3764
www.ajcr.us /ISSN:2156-6976/ajcr0122401

Original Article

TAS-102 has a tumoricidal activity in multiple myeloma

Guoli Li[1,2], Huan Liu[2,3], Jin He[2,3], Zongwei Li[2,3], Zhiming Wang[2,3], Shan Zhou[2,3], Guopei Zheng[1], Zhimin He[1], Jing Yang[2,3]

[1]Cancer Research Institute and Cancer Hospital, Guangzhou Medical University, Guangzhou, Guangdong, P. R. China; [2]Department of Lymphoma and Myeloma, Division of Cancer Medicine, The University of Texas MD Anderson Cancer Center, Houston, Texas 77030, USA; [3]Center for Hematologic Malignancy, Research Institute Houston Methodist Hospital, Houston, Texas 77030, USA

Received September 14, 2020; Accepted October 23, 2020; Epub November 1, 2020; Published November 15, 2020

Abstract: TAS-102/Lonsurf is a new oral anti-tumor drug consisting of trifluridine and tipiracil in a 1:0.5 molar ratio. Lonsurf has been approved globally, including US, Europe Union, and China, to treat patients with advanced colorectal cancer. Ongoing clinical trials are currently conducted for the treatment of other solid cancers. However, the therapeutic potential of TAS-102 in hematological malignancies has not been explored. In this study, we investigate the therapeutic efficacy of TAS-102 in multiple myeloma both *in vitro* and *in vivo*. We demonstrate that TAS-102 treatment inhibits tumor cell proliferation in six human myeloma cell lines with IC_{50} values in a range from 0.64 to 9.10 μM. Dot blotting and immunofluorescent staining show that trifluridine is predominately incorporated into genomic DNAs of myeloma cells. TAS-102 treatment induces myeloma cell apoptosis through cell cycle arrest in G1 phase and activation of cGAS-STING signaling in myeloma cells. In the human myeloma xenograft models, TAS-102 treatment reduces tumor progression and prolongs mouse survival. TAS-102 has shown its efficacies in the drug-resistant myeloma cells, and the combination of TAS-102 and bortezomib has a synergistic anti-myeloma activity. Our preclinical studies indicate that TAS-102 is a potential novel agent for myeloma therapy.

Keywords: Multiple myeloma, TAS-102, trifluridine, tipiracil, therapeutic effects

Introduction

Multiple myeloma is the second most common hematologic malignancy, which is caused by a malignant growth of clonal plasma cells in bone marrow [1]. International Agency for Research on Cancer estimated that in 2018, the global burden for this disease was approximately 159,985 newly diagnosed cases and 106,105 deaths [2]. In the past decades, there were great advancement in the treatment of multiple myeloma with the emergence of many novel chemotherapy agents, such as bortezomib, thalidomide, and lenalidomide, dramatically improved the overall survival for myeloma patients [3]. However, the majority of myeloma patients suffer from relapsed and refractory disease, and this malignancy remains an incurable disease [1]. Therefore, novel anti-myeloma drugs that improve patient outcomes are urgently warranted.

TAS-102 is a new oral antitumor drug developed by Taiho Oncology (Taiho Pharmaceutical Co., Ltd., Japan). It was first approved by the US Food and Drug Administration (FDA) in 2015, and then expanded globally including European Union and China for the treatment of patients with metastatic colorectal cancer [4, 5]. It was further approved by FDA for the treatment of patients with metastatic gastric or gastroesophageal junction adenocarcinoma in 2019. Other ongoing clinical trials of TAS-102 are mainly focused on solid tumors [6]. However, the antitumor activity of TAS-102 in hematologic malignancies, such as multiple myeloma, has not been reported.

TAS-102 is composed of two components: trifluridine and tipiracil at a molar ratio of 1:0.5 [7]. Trifluridine, an analog of thymidine that was firstly synthesized by Heidelberger and his colleagues [8], attributes to the anti-tumor cytotoxic potency of TAS-102 [6]. Trifluridine is phosphorylated by thymidine kinase 1 to its monophosphate form which inhibits thymidylate synthase, an enzyme that plays a central role in DNA synthesis [9]. Upon further phos-

phorylation, the monophosphate form turns into trifluridine triphosphate. The latter form can compete with thymidine bases to incorporate into DNA, thereby effectively interrupt DNA synthesis. Not surprisingly, the amount of trifluridine incorporation into DNAs has been shown to be positively correlated to its antitumor activity [10]. However, trifluridine is not very stable and can be rapidly degraded by thymidine phosphorylase [11]. The strategic combination of trifluridine with the hydrochloride tipiracil, an inhibitor of thymidine phosphorylase, greatly improves the bioavailability of trifluridine [6].

The efficacy of TAS-102 in cancer therapy attributes to the high expression of thymidine kinase 1 in cancer cells [12-14]. In multiple myeloma, the levels of thymidine kinase 1 expression are much high in malignant plasma cells and the elevated levels have served as a serum biomarker for poor prognosis in patients [15]. We thus hypothesized that TAS-102 might be an effective drug for the treatment of myeloma. In this preclinical study, we demonstrate that TAS-102 has a tumoricidal activity in myeloma *in vitro* and in the myeloma mouse model. Our study thus provides a rational basis for the future application of TAS-102 in clinical setting as a new agent for the treatment of myeloma patients.

Material and methods

Myeloma cell lines

Myeloma cell lines were purchased from American Type Culture Collection (ATCC), except ARP-1 cells, which was kindly provided by the University of Arkansas for Medical Sciences. The p53 knockout (KO) MM.1S cells and resistant myeloma cells against chemotherapeutic drugs were established as previously described before [16]. All myeloma cells were cultured in RPMI 1640 medium supplemented with 10% fetal bovine serum and 1% penicillin and streptomycin solution in a humidified incubator at 37°C with 5% CO_2.

Reagents and antibodies

TAS-102, Bortezomib (PS-341), and TPI were purchased from MedChemExpress LLC or Sigma Aldrich. Antibodies for western blot analysis were purchased from Cell Signaling Technology. Anti-BrdU antibody for dot blot assay was purchased from BD Biosciences. All siRNAs were purchased from Sigma-Aldrich.

MTS cell proliferation assay

Myeloma cell proliferation was determined by using CellTiter 96® AQueous Non-Radioactive Cell Proliferation Assay (Promega) according to the manufacture's protocol. Briefly, 1×10^3 cells/well were aliquoted into a 96-well opaque-walled plate and treated with TAS-102 alone or in combination with bortezomib for 72 hours. Wells without cells and with cell culture medium served as background control. The MTS/PMS solution was added, and incubated at 37°C for 3 hours. The absorbance at 490 nm were recorded using a plate reader (BioTek Instruments, Inc.).

Flow cytometry analysis

Annexin-V assay were used for analysis of apoptosis as described before [17]. Briefly, myeloma cells (1×10^5 cells/mL) were treated with various concentrations of TAS-102 for 72 hours and stained with fluorescein isothiocyanate-annexin V and propidium iodide. For cell cycle analysis, myeloma cells were first treated with or without 2 μM of TAS-102 for different lengths of time. Then the cells were fixed with 70% ice-cold ethanol, stained with 50 μg/mL propidium iodide supplemented with 20 μg/mL RNase. All samples were measured by a BD LSRFortessa flow cytometer and results were analyzed using FlowJo software.

The dot blot assay

Myeloma cells were cultured in the presence of 1 μM TAS-102 for different length of time (0, 2, 4, 6, and 12 hours). The assay was carried out as described previously [18]. Briefly, genomic DNA were isolated and then denatured with 0.1 N NaOH for 5 minutes at room temperature. Equal amounts of denatured genomic DNA were spotted onto nitrocellulose membrane that was situated in a Bio-Dot apparatus (Bio-Rad). The membranes were baked at 80°C, blocked with 5% BSA, and then blotted with anti-BrdU antibody (BD Biosciences) overnight at 4°C. The membrane was washed and incubated with a secondary antibody. To ensure equal spotting of DNA, the membrane was stained with 0.02% methylene blue in 0.3 M sodium acetate (pH 5.2).

Western blot analysis

Cells were harvested and lysed with 1 × lysis buffer (Cell Signaling Technologies). Cell lysates were subjected to SDS-PAGE, transferred to a nitrocellulose membrane, and immunoblotted with antibodies against Caspase 3, PARP, STING, cGAS, GAPDH, phosphorylated (p) or non-phosphorylated IRF3 and TBK1.

RNA extraction, reverse transcription, and quantitative real-time PCR

Total RNA was isolated using the Purelink RNA Mini Kit (Life Technologies). An aliquot of 0.5 μg of total RNA was subjected to reverse transcription with a SuperScript II RT-PCR kit (Life Technologies). Quantitative PCR was performed using SYBR Green Master Mix (Life Technologies) with the QuantStudio 3 Real-Time PCR System (Life Technologies). The primer sequences are as following: *TK1* forward: 5'-GGGCAGATCCAGGTGATTCTC-3', reverse: 5'-TGTAGCGAGTGTCTTTGGCATA-3'; *CDKN1A* forward: 5'-ATACCCTGTATGAAGGGAAGCC-3', reverse: 5'-CTTACCCCGAAGTTACGTCTTTC-3'; *GAPDH* forward: 5'-GCACCGTCAAGGCTGAGAAC-3', reverse: 5'-TGGTGAAGACGCCAGTGGA-3'.

Immunofluorescent staining

ARP-1 cells were treated with 2 μM TAS-102 for 24 hours and fixed with 4% paraformaldehyde. The fixed samples were then acid depurinated with 2 M HCl and 0.3% Triton-X 100 in 1 × PBS, incubated with anti-BrdU antibodies, and immunostained with Alexa Fluor 488-conjugated secondary antibodies. The cell nuclei were stained with 4',6-diamidino-2-phenylindole (DAPI). Immunofluorescence images were acquired using a Leica TCS SP8 confocal microscope system.

Myeloma xenograft mouse model

NOD-*scid* IL2rγ^{null} (NSG) mice were purchased from the Jackson Laboratory and maintained in American Association of Laboratory Animal Care–accredited facilities. The studies were approved by the Institutional Animal Care and Use Committee of the University of Texas MD Anderson Cancer Center. Six- to eight-week-old mice were injected intravenously with luciferase-labeled ARP-1 or MM.1S cells (5 × 10^5 cells/mouse). For *in vivo* studies, TAS-102 and vehicle were prepared in 0.5% hydroxypropyl methyl-cellulose (HPMC) as previously described [19]. After a week, TAS-102 (150 mg/kg/day) and vehicle (0.5% HPMC) were administrated to mice via oral gavage twice daily in a 5-day treatment/2-day drug-free routine during the course of the experiment. Weight of the mice were monitored regularly. Tumor burden was monitored at least weekly by levels of serum M-protein and strength of bioluminescent signal. Serum M-protein levels were measured by ELISA as described previously [20]. Bioluminescent signals were recorded by IVIS Spectrum In Vivo Imaging System and analyzed using Living Image Software (Perkin Elmer).

Combination effects

Myeloma cells were treated with a series of combinations with TAS-102 and bortezomib for 72 hours. The cell proliferation was measured, and combination index (CI) was calculated using CalcuSyn software (Biosoft version 2.0). CI <1 indicates synergism, whereas CI = 1 or >1 indicate additive effect or antagonism respectively [21, 22].

Statistical analysis

Statistical significance was analyzed using the GraphPad Prism software with two tailed unpaired Student *t*-tests for comparison of two groups, and one-way ANOVA with Tukey's multiple comparisons test for comparison of more than two groups. *P* values less than 0.05 were considered statistically significant. All results were reproduced in at least three independent experiments.

Results

TAS-102 treatment inhibits proliferation and induces apoptosis in myeloma cells

High expression of thymidine kinase 1 in cancer cells is essential for the sensitivity of trifluridine treatment [13]. The malignant plasma cells in myeloma patients highly express this kinase [15], and we confirmed the upregulation of this kinase in most of the tested human myeloma cell lines (**Figure 1A**), indicating the potential of TAS-102 in the treatment of multiple myeloma. To investigate the effect of TAS-102 on proliferation, the human myeloma cell lines ARP-1, JJN3, MM.1S, NCI-H929, OPM-2 and U266 were cultured in medium with vari-

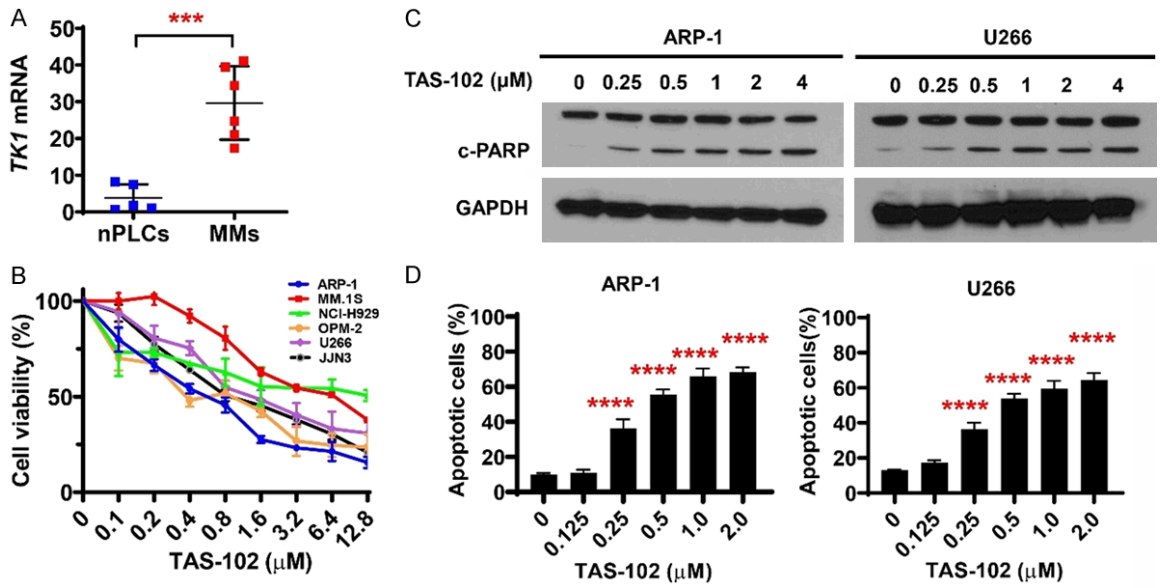

Figure 1. Treatment of TAS-102 inhibits proliferation and induces apoptosis in myeloma cells. (A) Relative expression of thymidine kinase 1 (*TK1*) mRNA in 6 myeloma cell lines (MMs: ARP-1, MM.1S, ARK, H929, U266, and RPMI8266). Expression of normal plasma cells (nPLCs, n = 5) served as control. (B) Shown is the viability of myeloma cells treated with different doses of TAS-102. Myeloma cells were cultured with various concentrations of TAS-102 for 3 days, and the cell viability were evaluated using MTS assay. The cells without TAS-102 treatment (0) served as controls. (C) Western blotting shows the levels of cleaved PARP (c-PARP) in myeloma cells treated without (0, as controls) or with TAS-102 for 36 hours. (D) Shown are the percentage of apoptotic myeloma cells treated with different doses of TAS-102. Myeloma cell lines ARP-1 or U266 were cultured without (0, as controls) or with TAS-102 (0.125, 0.25, 0.5, 1.0 or 2 μM) for 3 days, and the percentage of apoptotic myeloma cells was determined by Annexin-V assay. Images in (C) are representatives of 3 independent experiments. Data are means ± SD from n = 3 independent experiments. ***P<0.001; ****P<0.0001. P values were determined using student's t test for paired samples and one-way ANOVA with Tukey's multiple comparisons test for more than two samples.

ous concentrations of TAS-102 for 72 hours, and then analyzed using the CellTiter 96® Aqueous Non-Radioactive Assay kit for cellular viability. Cells without TAS-102 treatment served as controls. As shown in **Figure 1B**, the treatment of TAS-102 dramatically reduced the viabilities of myeloma cells in a dose-dependent manner. The half-maximal inhibitory concentration (IC_{50}) was 0.64 μM for ARP-1, 0.79 μM for JJN3, 4.49 μM for MM.1S, 9.10 μM for NCI-H929, 0.65 μM for OPM-2, or 2.15 μM for U266 cells, respectively. These results indicate that TAS-102 treatment inhibits myeloma cell proliferation *in vitro*.

We next investigated the effects of TAS-102 on myeloma cell apoptosis. Treatment of myeloma ARP-1 or U266 cells with TAS-102 for 36 hours increased the cleavage of PARP, a marker of cellular apoptosis, in a dose-dependent manner (**Figure 1C**). After the 72 hour-incubation with various concentrations of TAS-102, we found the increased percentage of apoptotic myeloma ARP-1 or U266 cells comparing to those without the treatment (**Figure 1D**). Because antibodies against bromodeoxyuridine/5-bromo-2'-deoxyuridine (BrdU) can specifically recognize the incorporation of trifluridine into DNA [18, 23], we performed dot blot and immunofluorescent staining using anti-BrdU antibodies to evaluate the effect of TAS-102 on DNA incorporation in myeloma cells. The results from dot blotting showed that the amounts of trifluridine DNA incorporation in ARP-1 cells were increased in a time-dependent manner after TAS-102 treatment (**Figure 2A**). The trifluridine incorporation into DNA was also confirmed by immunofluorescent staining (**Figure 2B**). Since DNA damage-induced cell apoptosis is mainly through the p21/p53-dependent cell cycle arrest [24, 25], we wondered whether TAS-102 has an effect on the cell cycle of myeloma cells. Propidium iodide staining showed that TAS-102 treatment caused MM.1S or U266 cells into G1 phase (**Figure 2C**). The treatment also induced time-dependent increase of *CDKN1A* mRNAs, the gene encoding p21, in myeloma MM.1S, U266,

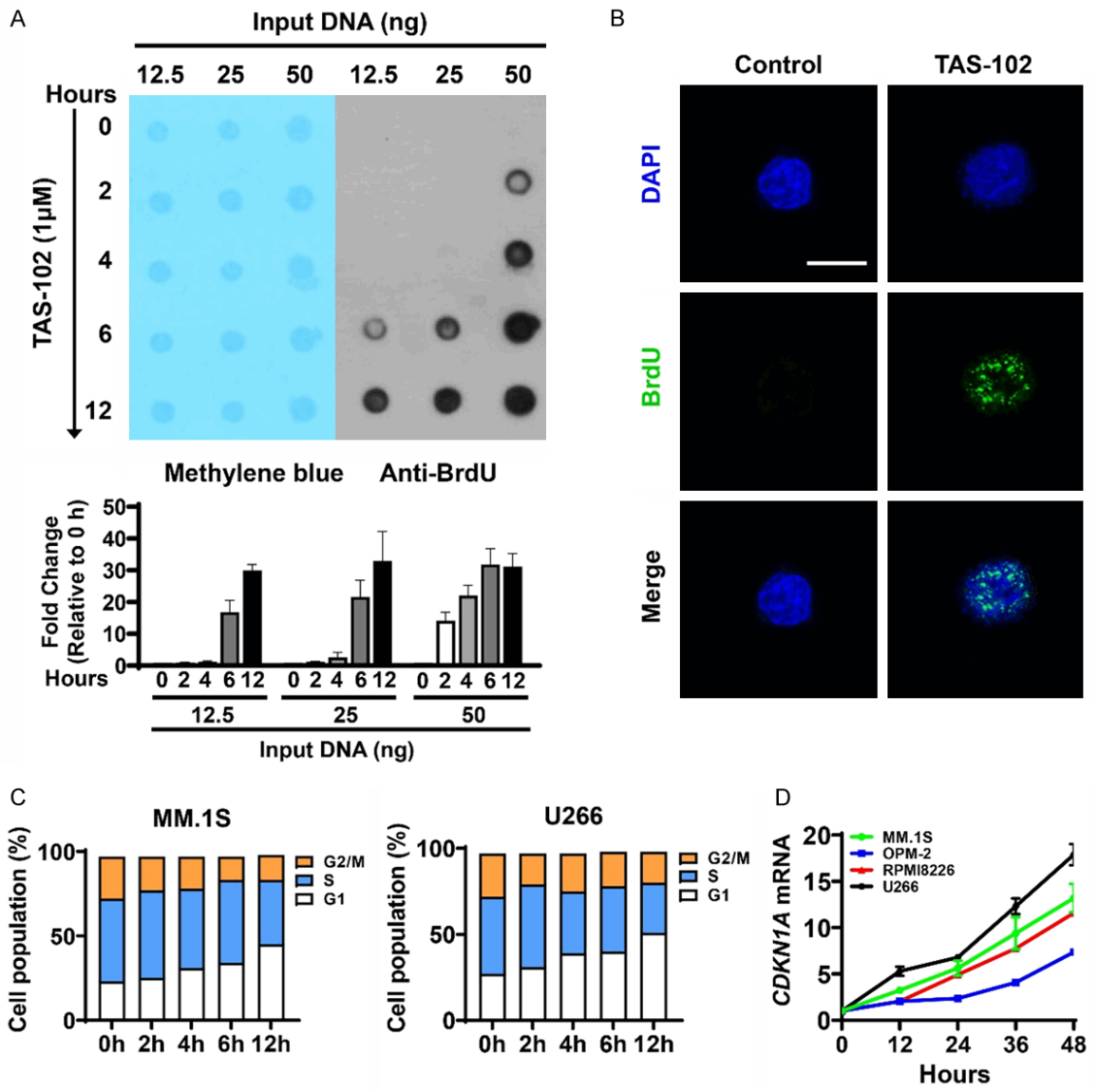

Figure 2. TAS-102 treatment induces trifluridine incorporation into DNAs and cell cycle arrest in myeloma cells. (A) Dot blot analysis shows trifluridine incorporation into the DNAs of myeloma ARP-1 cells. ARP-1 cells were cultured with TAS-102 for 0 (controls), 2, 4, 6, or 12 hours (h). The purified DNAs were denatured, spotted onto nitrocellulose membrane, and immunoblotted with anti-BrdU antibody. The relative fold change on the incorporated DNAs after TAS-102 treatment are shown in the lower panel. The amount of incorporated DNAs at hour 0 is set to 1. (B) Representative immunofluorescent images show trifluridine incorporation detected by confocal microscopy. Myeloma ARP-1 cells were cultured in the presence of 1 μM TAS-102 for 12 hours, and then immunostained with the anti-BrdU antibody and Alexa Fluor 488-conjugared secondary antibody. Nuclei were counterstained with DAPI. Scale Bar: 5 μm. Experiments. Images are representatives of 3 independent experiments. (C) Shown is the percentage of cell populations in G2/M, S, or G1 phase of cell cycle. MM.1S and U266 cells were treated with 2 μM TAS-102 for 0 (as controls), 2, 4, 6, or 12 hours (h). Fixed cells were stained with PI and DNA content were analyzed by flow cytometry. (D) qPCR analysis shows the relative expression of *CDKN1A* mRNAs in MM.1S, OPM2, RPMI8226, or U266 cells that were treated with 1 μM TAS-102 for 0 (controls), 12, 24, 36, or 48 hours (h).

OPM-2, and RPMI8226 cells (**Figure 2D**). Together, our results indicate that treatment of TAS-102 inhibits myeloma cell proliferation, induces myeloma cell apoptosis and cell cycle arrest *in vitro*.

TAS-102 induces myeloma cells apoptosis through the cGAS-STING pathway

In **Figure 1**, we found that TAS-102 treatment also induced apoptosis in the p53-null myelo-

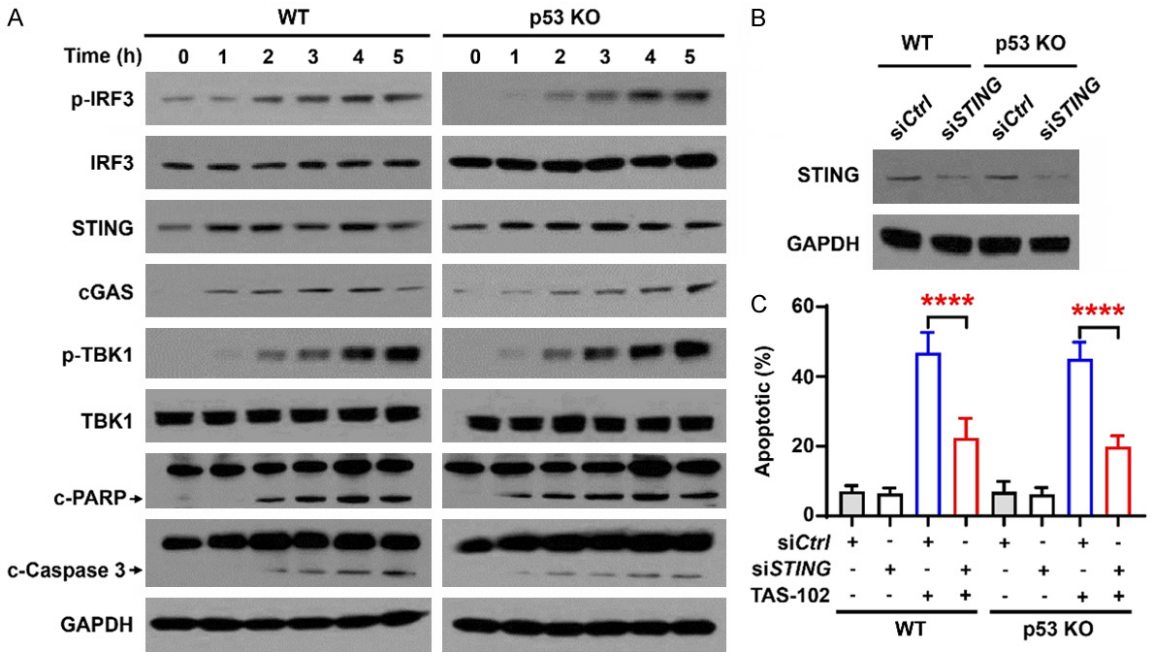

Figure 3. TAS-102 induces myeloma cells apoptosis through cGAS-STING pathways. MM.1S wild type (WT) or MM.1S p53 KO cells were treated without or with 5 μM of TAS-102 for 0 (controls), 1, 2, 3, 4 or 5 hours (h). Shown are the levels of cGAS, STING, cleaved PARP, cleaved Caspase 3, phosphorylated IRF3 and TBK1, non-phosphorylated TBK1 and IRF3. GAPDH levels served as protein loading controls (A). (B) Western blotting showing the expression of STING in myeloma cells transfected with STING siRNAs (si*STING*). Nontargeted siRNA (si*Ctrl*)-expressing myeloma cells served as controls. (C) Shown are the percentage of apoptotic myeloma cells treated with or without TAS-102 (1 μM) for 2 days in different siRNA transfected groups. The percentage of apoptotic myeloma cells was determined by Annexin-V assay. Data are averages ± SD. Each experiment was repeated three times. ****P<0.0001. All P values were determined using one-way ANOVA.

ma cells ARP-1 and JJN3 [26], which indicated that there might be other signaling pathways involved in TAS-102 induced myeloma cell apoptosis. Previous studies have shown that the cytosolic DNA sensing cGAS-STING pathway is greatly important for the cells in response to DNA damage [27]. This pathway can promote cellular apoptosis through the transcriptional activation of apoptotic regulators as well as through a transcription-independent role of IRF3 [28]. We observed that the expression level of cGAS, STING, the cleaved level of PARP, Caspase 3, and the phosphorylated level of IRF3, TBK1 were upregulated in either wide-type MM.1S myeloma cells or the p53-knock-out cells (MM.1S p53 KO), while the level of non-cleaved PARP, Caspase 3, the level of non-phosphorylated TBK1, IRF3 were not changed, and the level of GAPDH protein served as protein loading controls (**Figure 3A**). We next knocked down STING expression in wild type or MM.1S p53 KO myeloma cells using the specific small interfering RNAs (siRNAs) against *STING* (si*STING*). We observed the reduced apoptosis in the si*STING* myeloma cells, compared with that in si*Ctrl* cells, after TAS-102 treatment (**Figure 3B** and **3C**). These results indicate an additional mechanism of TAS-102-induced myeloma cell apoptosis through activation of the cGAS-STING pathway.

TAS-102 treatment reduces myeloma growth in the myeloma xenograft mouse model

To investigate the anti-myeloma activity of TAS-102 *in vivo*, we used a human myeloma xenograft model. We intravenously injected mice with luciferase-labeled myeloma ARP-1 or MM.1S cells, and treated the mice with TAS-102 (150 mg/kg/day) via oral gavage. The tumor burden was monitored by bioluminescent imaging and serum M-protein levels. As the bioluminescent signals progressed over time in the control mice injected with myeloma cells, we found a significant decrease of bioluminescent intensity in mice treated with TAS-102 (**Figure 4A** and **4B**). In addition, we collected serum from mice weekly, and exam-

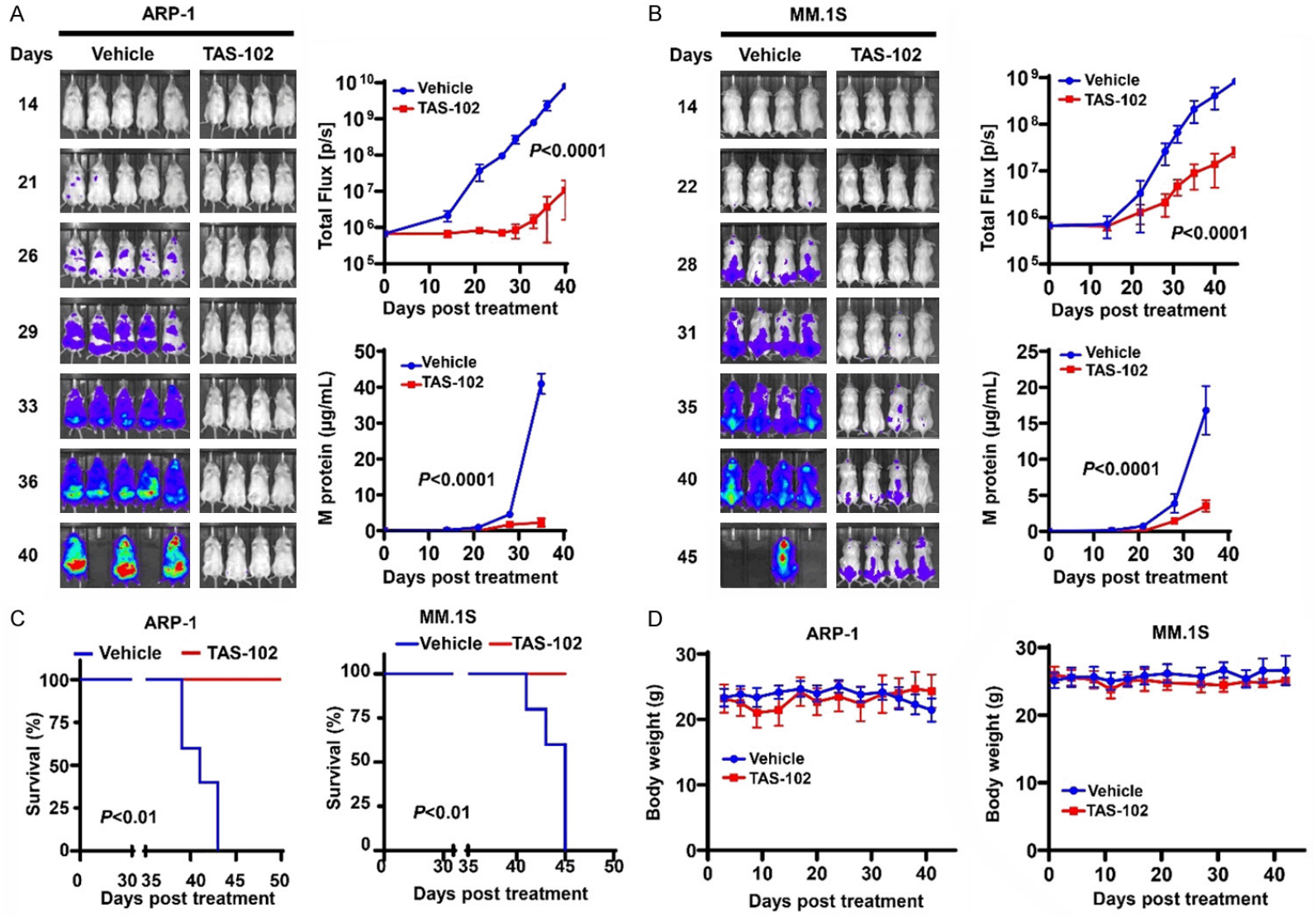

Figure 4. TAS-102 reduces myeloma growth and prolongs survival in the myeloma xenograft model. (A, B) NSG mice were intravenously injected with luciferase-labeled ARP-1 or MM.1S cells. After 1 week, mice were treated with TAS-102 (150 mg/kg/day) or vehicle control via oral gavage twice daily five days a week. Tumor burden was monitored by bioluminescent imaging and serum M-protein level. Shown are representative images, summarized data, and M-protein levels in mice injected with ARP-1 (A) or MM.1S cells (B) post TAS-102 treatment. (C) Shown is the survival curve of myeloma bearing mice with or without TAS-102 treatment. (D) Shown is the body weight of mice during the treatment. Results shown as averages ± SD (n = 4-5 mice/group) were representative of three replicate studies. *P* values were determined using the Student *t*-test.

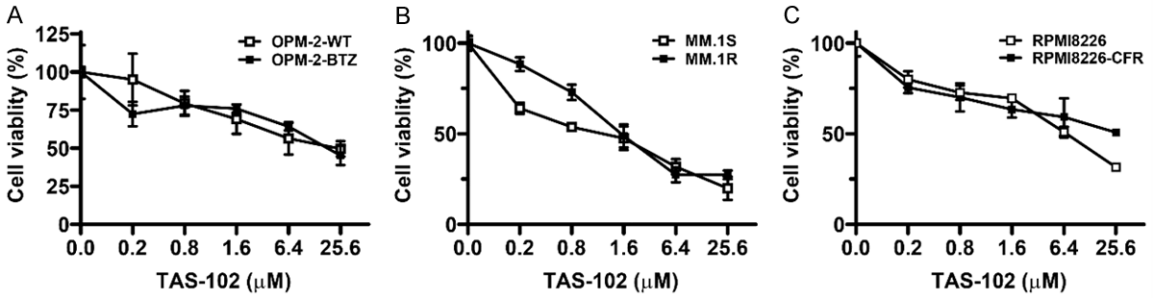

Figure 5. TAS-102 has an anti-myeloma activity in chemo-resistant myeloma cells. Wild-type/parental myeloma cells and their respective chemo-resistant cells were treated with various concentrations of TAS-102 for 72 hours. Cells without the treatment served as controls. Shown are the cell viabilities in (A) bortezomib-sensitive OPM-2 (OPM-2-WT) and bortezomib-resistant OPM-2 BTZ (OPM-2-BTZ), (B) dexamethasone-sensitive MM.1S and dexamethasone-resistant MM.1R, and (C) carfilzomib-sensitive RPMI8226 and carfilzomib-resistant RPMI8226 (RPMI8226-CFR) cells. Data are averages ± SD from three independent experiments.

ined the circulating M-protein concentration using ELISA. Our results showed that the levels of M-proteins were remarkedly reduced in TAS-102 treated mice comparing to those in control mice (**Figure 4A** and **4B**). Furthermore, TAS-102 treatment dramatically prolonged survival of mice (**Figure 4C**). These results indicate the therapeutic efficacy of TAS-102 in myeloma *in vivo*. In addition, we did not observe significant weight loss in the treatment group as compared with those in control groups (**Figure 4D**), suggesting that the current dose used in the TAS-102 treatment has little toxicity and it is a safe dose for mice.

TAS-102 treatment has a tumoricidal activity in chemo-resistant myeloma cells

The proteasome inhibitors bortezomib, carfilzomib, and the traditional chemotherapy drug dexamethasone are commonly used in myeloma. However, majority of the patients suffer from relapses due to the drug resistance. We wondered whether TAS-102 could overcome such resistance. We added various doses of TAS-102 to the cultures of the paired parental and drug-resistant myeloma cells, which include the OPM-2 wild type (OPM-2-WT) and bortezomib-resistant (OPM-2-BTZ) cell lines (**Figure 5A**), the dexamethasone-sensitive (MM.1S) and -resistant (MM.1R) cell lines (**Figure 5B**), and the RPMI8226 wild type and carfilzomib-resistant (RPMI8226-CFZ) cell lines (**Figure 5C**). MTS assay showed that TAS-102 treatment significantly reduced the viability of either parental or drug-resistant myeloma cells, and there was no difference in the reduction of viability between parental and resistant cells, indicating that TAS-102 also exerts anti-myeloma activity in those cells against common therapies.

Combination of bortezomib and TAS-102 has a synergistic therapeutic effect in myeloma

Combination therapy often offers synergistic anti-myeloma effects and it is commonly used in myeloma patients [10, 29]. Since trifluridine induces cell cycle arrest in solid tumors is proteasome-dependent [30], we hypothesized that TAS-102 might trigger an synergistic anti-myeloma activity when it is combined with proteasome inhibitors, such as bortezomib, a frontline drug for myeloma patients. To assess the combined efficacy, myeloma ARP-1 and U266 cells were treated with the compound alone or in a combination of the two. The cells without treatment served as controls. MTS assay was performed to determine the cell viability, and the antagonism or synergism of the combination was evaluated using Chou-Talalay analysis [21, 22]. Our results showed that combination of TAS-102 and bortezomib displayed a synergic effect on reduction of viability in ARP-1 (**Figure 6A**) and U266 (**Figure 6B**) cells with a combination index (CI) <1.0, indicating that combination with TAS-102 improve the efficacy of current chemotherapy drugs, such as bortezomib, in myeloma.

Discussion

TAS-102 is a new drug that has been used in patients with gastrointestinal tumors [31]. In this study, we extend its application to hematological malignancy - multiple myeloma. We

A

ARP-1

Combination	TAS102 (μM)	Fa (TAS-102)	BTZ (nM)	Fa (BTZ)	Fa (Com.)	CI
1	0.5	0.315	4	0.341	0.545	0.55505
2	0.5	0.315	8	0.460	0.803	0.13085
3	0.5	0.315	16	0.562	0.865	0.10979
4	1.0	0.486	4	0.341	0.581	0.66242
5	1.0	0.486	8	0.460	0.897	0.05522
6	1.0	0.486	16	0.562	0.893	0.08823
7	2.0	0.573	4	0.341	0.691	0.53488
8	2.0	0.573	8	0.460	0.843	0.17199
9	2.0	0.573	16	0.562	0.915	0.08015

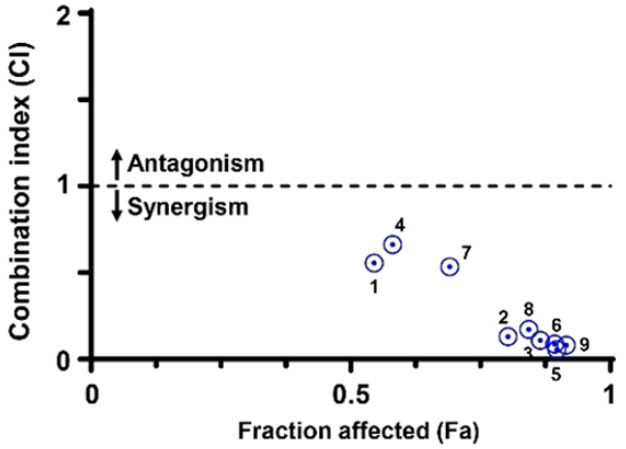

B

U266

Combination	TAS102 (μM)	Fa (TAS-102)	BTZ (nM)	Fa (BTZ)	Fa (Com.)	CI
1	0.5	0.278	4	0.280	0.403	1.08344
2	0.5	0.278	8	0.588	0.607	0.82197
3	0.5	0.278	16	0.670	0.774	0.76740
4	1.0	0.308	4	0.280	0.547	0.74330
5	1.0	0.308	8	0.588	0.687	0.65674
6	1.0	0.308	16	0.670	0.820	0.61993
7	2.0	0.490	4	0.280	0.606	0.77873
8	2.0	0.490	8	0.588	0.759	0.53616
9	2.0	0.490	16	0.670	0.834	0.60345

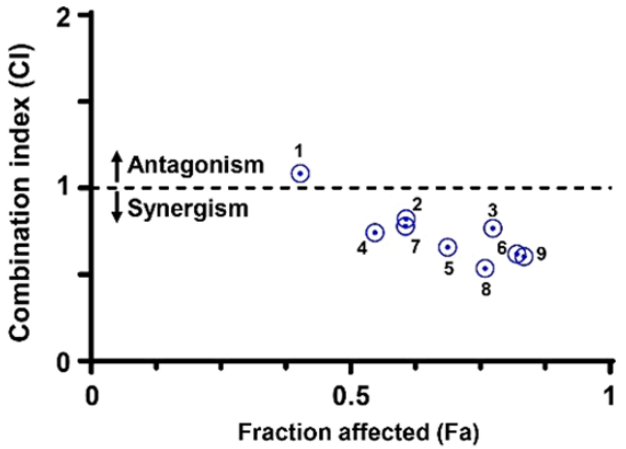

Figure 6. Combination of TAS-102 and bortezomib has a synergistic anti-myeloma activity. ARP-1 (A) or U266 (B) cells were treated with TAS-102 and bortezomib for 72 hours, and then assessed for viability using MTS assay. The synergistic cytotoxic effect of TAS-102 and bortezomib were analyzed using Chou-Talalay assays. Combination index (CI) <1 indicates synergy.

demonstrate that TAS-102 has the anti-myeloma activities *in vitro* and *in vivo* through reduction of proliferation, induction of apoptosis, and cell cycle arrest in myeloma cells. We also explore the potential application of TAS-102 to improve current myeloma therapy by overcoming drug resistance and by combination chemotherapy regimens.

Although the exact mechanism of TAS-102 induced cytotoxicity is still unclear, both the inhibitory effects on thymidylate synthase activity in its monophosphate form and the incorporation into DNAs in its triphosphate form can cause cytotoxicity in solid tumors [9]. Like that in colorectal cancer, we found trifluridine can induce DNA incorporation in myeloma cells and activate cGAS-STING signaling pathway, leading to myeloma cell death. In addition, we found that the treatment of TAS-102 induced cell cycle arrest at G1 phase in myeloma cells. These findings are different from previous studies conducted in colorectal cancer showing that trifluridine induces cell cycle arrest at G2 phase [30]. The cell cycle arrest in myeloma cells induced by TAS-102 is associated with the upregulation of p21 expression. The p21 is a well-known inhibitor of cell cycle in the tumor-suppressor p53-dependent manner upon DNA damage, which influences cell cycle progression in both G1/S transition and G2/M phase through inhibition of CDK4, 6/cyclin-D or CDK2/cyclin-E, respectively [32]. The efficacy of the DNA damage checkpoint machinery at the p21-dependent G1/S boundary in hematological malignancies is different from solid tumors [33, 34]. Thus, such difference may partially explain why the cell cycle of TAS-102 treated myeloma cells is arrested at G1 but not at G2. Our future study will further investigate how TAS-102 induces the p21-dependent G1 arrest in myeloma and other hematological malignancies. In addition, we have investigated the p53-independent cell cycle arrest in myeloma cells induced by TAS-102. The drugs damaging DNAs induce tumor cell apoptosis mainly in a p53-dependent manner. However, p53 protein is frequently deleted in patients with multiple myeloma [35]. We investigated the cGAS-STING pathway in TAS-102 treated myeloma cells, since the cGAS-STING is a DNA damage sensor [28]. Our results have identified a new p53-independent way to induce apoptosis in p53-null myeloma cells through activation of the cGAS-STING pathway.

The effective combination of TAS-102 with conventional chemotherapy drugs has been widely investigated in colon and gastric cancers [11], and we confirm the synergistic effect of TAS-102 and bortezomib combination in myeloma. We found that the combination of bortezomib with TAS-102 was more effective than bortezomib treatment alone in myeloma. We also found that TAS-102 treatment had a similar effect on apoptosis in either wild-type or resistant myeloma cells against bortezomib, carfilzomib, and dexamethasone that are commonly used in myeloma therapy. These findings suggest a rationale for the potential clinical benefit of TAS-102 to improve the current chemotherapy in myeloma patients.

We also demonstrated the tumoricidal activity of TAS-102 *in vivo*, since we found the drastically reduced tumor burden in myeloma-bearing mice with little toxicity during our observation. Another benefit of TAS-102 application is its therapeutic potential in myeloma-associated bone disease. Besides its ability to stabilize trifluridine, tipiracil, which is the other key component of TAS-102, is an inhibitor against thymidine phosphorylase [6, 11]. Our previous studies have demonstrated that myeloma cells highly express thymidine phosphorylase which has a functional role in myeloma-induced bone lesions through the 2DDR-mediated signaling pathways [36]. Osteolytic lesions are a hallmark of multiple myeloma [37-39]. More than 80% of patients with myeloma develop lytic lesions in bone, which causes pathological fractures, severe bone pain, spinal cord compression and hypercalcemia, and therefore impairs the quality of patient life. We have used tipiracil in myeloma mouse models and found the significant reduction of osteoclast-mediated bone resorption and increase of osteoblast-mediated bone formation [36], indicating the application of tipiracil is a new viable therapeutic option for treatment of myeloma patients with bone lesions. Bone marrow microenvironment, where myeloma cell resides, has been shown to foster myeloma growth and induction of myeloma drug resistance, because the lytic bone releases of many growth factors. Thus, prevention of thymidine phosphorylase-induced myeloma bone lesions may be also beneficial for improve the outcomes of myeloma patients. In our future studies, we will examine the therapeutic efficacy of tipiracil alone or TAS-102 on myeloma bone disease and their impact on

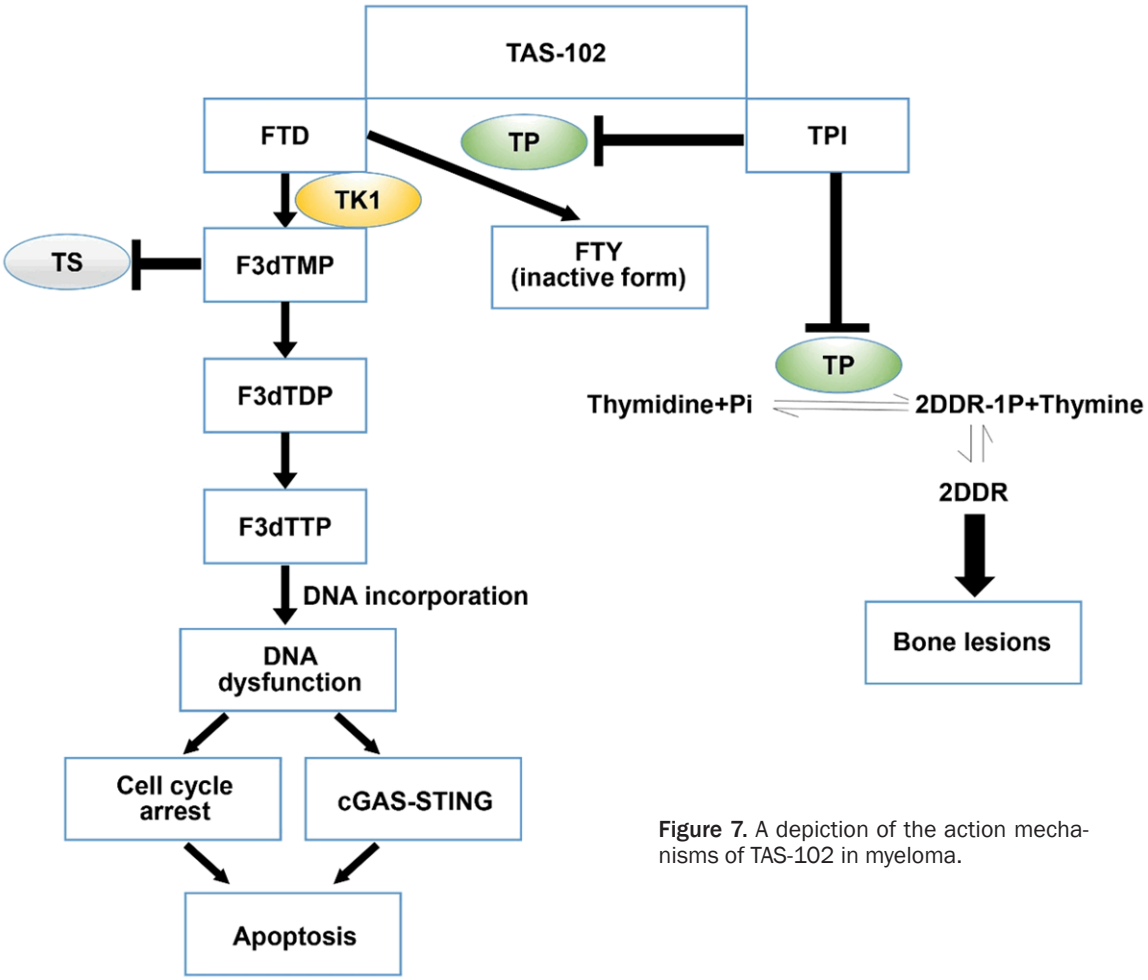

Figure 7. A depiction of the action mechanisms of TAS-102 in myeloma.

marrow microenvironment-induced myeloma growth and survival. We believe that patients with multiple myeloma may be potentially benefited from TAS-102 in two major aspects: killing tumor cells and healing lytic lesions (**Figure 7**).

Overall, our preclinical studies demonstrate the anti-myeloma activity of TAS-102 and implicate the potential clinical application of TAS-102 as a novel promising drug for multiple myeloma therapy alone or in a combination with current chemotherapy. Evaluation of TAS-102 in the treatment of myeloma patients in clinical trials is necessary for investigation.

Acknowledgements

We thank the Small Animal Imaging Facility and Advanced Microscopy Core Facility, which are core labs from University of Texas MD Anderson Cancer Center.

Disclosure of conflict of interest

None.

Address correspondence to: Drs. Huan Liu and Jing Yang, Center for Hematologic Malignancy, Research Institute Houston Methodist Hospital, Houston, Texas 77030, USA. E-mail: bjx-2002@163.com (HL); jyang2@houstonmethodist.org (JY)

References

[1] Röllig C, Knop S and Bornhäuser M. Multiple myeloma. Lancet 2015; 385: 2197-2208.

[2] Bray F, Ferlay J, Soerjomataram I, Siegel RL, Torre LA and Jemal A. Global cancer statistics 2018: GLOBOCAN estimates of incidence and mortality worldwide for 36 cancers in 185 countries. CA Cancer J Clin 2018; 68: 394-424.

[3] Kumar SK, Dispenzieri A, Lacy MQ, Gertz MA, Buadi FK, Pandey S, Kapoor P, Dingli D, Hayman SR, Leung N, Lust J, McCurdy A, Russell

SJ, Zeldenrust SR, Kyle RA and Rajkumar SV. Continued improvement in survival in multiple myeloma: changes in early mortality and outcomes in older patients. Leukemia 2014; 28: 1122-1128.

[4] Shitara K, Doi T, Dvorkin M, Mansoor W, Arkenau HT, Prokharau A, Alsina M, Ghidini M, Faustino C, Gorbunova V, Zhavrid E, Nishikawa K, Hosokawa A, Yalcin S, Fujitani K, Beretta GD, Van Cutsem E, Winkler RE, Makris L, Ilson DH and Tabernero J. Trifluridine/tipiracil versus placebo in patients with heavily pretreated metastatic gastric cancer (TAGS): a randomised, double-blind, placebo-controlled, phase 3 trial. Lancet Oncol 2018; 19: 1437-1448.

[5] Mayer RJ, Van Cutsem E, Falcone A, Yoshino T, Garcia-Carbonero R, Mizunuma N, Yamazaki K, Shimada Y, Tabernero J, Komatsu Y, Sobrero A, Boucher E, Peeters M, Tran B, Lenz HJ, Zaniboni A, Hochster H, Cleary JM, Prenen H, Benedetti F, Mizuguchi H, Makris L, Ito M and Ohtsu A. Randomized trial of TAS-102 for refractory metastatic colorectal cancer. N Engl J Med 2015; 372: 1909-1919.

[6] Uboha N and Hochster HS. TAS-102: a novel antimetabolite for the 21st century. Future Oncol 2016; 12: 153-163.

[7] Emura T, Murakami Y, Nakagawa F, Fukushima M and Kitazato K. A novel antimetabolite, TAS-102 retains its effect on FU-related resistant cancer cells. Int J Mol Med 2004; 13: 545-549.

[8] Heidelberger C, Parsons DG and Remy DC. Syntheses of 5-trifluoromethyluracil and 5-trifluoromethyl-2'-deoxyuridine. J Med Chem 1964; 7: 1-5.

[9] Lenz HJ, Stintzing S and Loupakis F. TAS-102, a novel antitumor agent: a review of the mechanism of action. Cancer Treat Rev 2015; 41: 777-783.

[10] Peeters M, Cervantes A, Moreno Vera S and Taieb J. Trifluridine/tipiracil: an emerging strategy for the management of gastrointestinal cancers. Future Oncol 2018; 14: 1629-1645.

[11] Peters GJ. Therapeutic potential of TAS-102 in the treatment of gastrointestinal malignancies. Ther Adv Med Oncol 2015; 7: 340-356.

[12] Emura T, Nakagawa F, Fujioka A, Ohshimo H and Kitazato K. Thymidine kinase and thymidine phosphorylase level as the main predictive parameter for sensitivity to TAS-102 in a mouse model. Oncol Rep 2004; 11: 381-387.

[13] Kataoka Y, Iimori M, Niimi S, Tsukihara H, Wakasa T, Saeki H, Oki E, Maehara Y and Kitao H. Cytotoxicity of trifluridine correlates with the thymidine kinase 1 expression level. Sci Rep 2019; 9: 7964.

[14] Shintani M, Urano M, Takakuwa Y, Kuroda M and Kamoshida S. Immunohistochemical characterization of pyrimidine synthetic enzymes, thymidine kinase-1 and thymidylate synthase, in various types of cancer. Oncol Rep 2010; 23: 1345-1350.

[15] Brown RD, Joshua DE, Ioannidis RA and Kronenberg H. Serum thymidine kinase as a marker of disease activity in patients with multiple myeloma. Aust N Z J Med 1989; 19: 226-232.

[16] Lee HC, Wang H, Baladandayuthapani V, Lin H, He J, Jones RJ, Kuiatse I, Gu D, Wang Z, Ma W, Lim J, O'Brien S, Keats J, Yang J, Davis RE and Orlowski RZ. RNA polymerase I inhibition with CX-5461 as a novel therapeutic strategy to target MYC in multiple myeloma. Br J Haematol 2017; 177: 80-94.

[17] Tu YS, He J, Liu H, Lee HC, Wang H, Ishizawa J, Allen JE, Andreeff M, Orlowski RZ, Davis RE and Yang J. The imipridone ONC201 induces apoptosis and overcomes chemotherapy resistance by up-regulation of bim in multiple myeloma. Neoplasia 2017; 19: 772-780.

[18] Kitao H, Morodomi Y, Niimi S, Kiniwa M, Shigeno K, Matsuoka K, Kataoka Y, Iimori M, Tokunaga E, Saeki H, Oki E and Maehara Y. The antibodies against 5-bromo-2'-deoxyuridine specifically recognize trifluridine incorporated into DNA. Sci Rep 2016; 6: 25286.

[19] Suzuki N, Tsukihara H, Nakagawa F, Kobunai T and Takechi T. Synergistic anticancer activity of a novel oral chemotherapeutic agent containing trifluridine and tipiracil in combination with anti-PD-1 blockade in microsatellite stable-type murine colorectal cancer cells. Am J Cancer Res 2017; 7: 2032-2040.

[20] Zhang M, He J, Liu Z, Lu Y, Zheng Y, Li H, Xu J, Liu H, Qian J, Orlowski RZ, Kwak LW, Yi Q and Yang J. Anti-β2-microglobulin monoclonal antibodies overcome bortezomib resistance in multiple myeloma by inhibiting autophagy. Oncotarget 2015; 6: 8567-78.

[21] Chou TC. Drug combination studies and their synergy quantification using the Chou-Talalay method. Cancer Res 2010; 70: 440-446.

[22] Zhang N, Fu JN and Chou TC. Synergistic combination of microtubule targeting anticancer fludelone with cytoprotective panaxytriol derived from panax ginseng against MX-1 cells in vitro: experimental design and data analysis using the combination index method. Am J Cancer Res 2016; 6: 97-104.

[23] Nakanishi R, Kitao H, Kiniwa M, Morodomi Y, Iimori M, Kurashige J, Sugiyama M, Nakashima Y, Saeki H, Oki E and Maehara Y. Monitoring trifluridine incorporation in the peripheral blood mononuclear cells of colorectal cancer patients under trifluridine/tipiracil medication. Sci Rep 2017; 7: 16969.

[24] Lane DP. Cancer. p53, guardian of the genome. Nature 1992; 358: 15-16.

[25] Levine AJ. p53, the cellular gatekeeper for growth and division. Cell 1997; 88: 323-331.
[26] Xiong W, Wu X, Starnes S, Johnson SK, Haessler J, Wang S, Chen L, Barlogie B, Shaughnessy JD Jr and Zhan F. An analysis of the clinical and biologic significance of TP53 loss and the identification of potential novel transcriptional targets of TP53 in multiple myeloma. Blood 2008; 112: 4235-4246.
[27] Li T and Chen ZJ. The cGAS-cGAMP-STING pathway connects DNA damage to inflammation, senescence, and cancer. J Exp Med 2018; 215: 1287-1299.
[28] Zierhut C, Yamaguchi N, Paredes M, Luo JD, Carroll T and Funabiki H. The cytoplasmic DNA sensor cGAS promotes mitotic cell death. Cell 2019; 178: 302-315, e323.
[29] Manasanch EE and Orlowski RZ. Proteasome inhibitors in cancer therapy. Nat Rev Clin Oncol 2017; 14: 417-433.
[30] Matsuoka K, Iimori M, Niimi S, Tsukihara H, Watanabe S, Kiyonari S, Kiniwa M, Ando K, Tokunaga E, Saeki H, Oki E, Maehara Y and Kitao H. Trifluridine induces p53-dependent sustained G2 phase arrest with its massive misincorporation into DNA and few DNA strand breaks. Mol Cancer Ther 2015; 14: 1004-1013.
[31] Marcus L, Lemery SJ, Khasar S, Wearne E, Helms WS, Yuan W, He K, Cao X, Yu J, Zhao H, Wang Y, Stephens O, Englund E, Agarwal R, Keegan P and Pazdur R. FDA approval summary: TAS-102. Clin Cancer Res 2017; 23: 2924-2927.
[32] Georgakilas AG, Martin OA and Bonner WM. p21: a two-faced genome guardian. Trends Mol Med 2017; 23: 310-319.
[33] Ashraf HM, Moser J and Spencer SL. Senescence evasion in chemotherapy: a sweet spot for p21. Cell 2019; 178: 267-269.
[34] Hsu CH, Altschuler SJ and Wu LF. Patterns of early p21 dynamics determine proliferation-senescence cell fate after chemotherapy. Cell 2019; 178: 361-373, e12.
[35] Drach J, Ackermann J, Fritz E, Kromer E, Schuster R, Gisslinger H, DeSantis M, Zojer N, Fiegl M, Roka S, Schuster J, Heinz R, Ludwig H and Huber H. Presence of a p53 gene deletion in patients with multiple myeloma predicts for short survival after conventional-dose chemotherapy. Blood 1998; 92: 802-809.
[36] Liu H, Liu Z, Du J, He J, Lin P, Amini B, Starbuck MW, Novane N, Shah JJ, Davis RE, Hou J, Gagel RF and Yang J. Thymidine phosphorylase exerts complex effects on bone resorption and formation in myeloma. Sci Transl Med 2016; 8: 353ra113.
[37] He J, Liu Z, Zheng Y, Qian J, Li H, Lu Y, Xu J, Hong B, Zhang M, Lin P, Cai Z, Orlowski RZ, Kwak LW, Yi Q and Yang J. p38 MAPK in myeloma cells regulates osteoclast and osteoblast activity and induces bone destruction. Cancer Res 2012; 72: 6393-6402.
[38] Terpos E, Ntanasis-Stathopoulos I and Dimopoulos MA. Myeloma bone disease: from biology findings to treatment approaches. Blood 2019; 133: 1534-1539.
[39] Yang J, He J, Wang J, Cao Y, Ling J, Qian J, Lu Y, Li H, Zheng Y, Lan Y, Hong S, Matthews J, Starbuck MW, Navone NM, Orlowski RZ, Lin P, Kwak LW and Yi Q. Constitutive activation of p38 MAPK in tumor cells contributes to osteolytic bone lesions in multiple myeloma. Leukemia 2012; 26: 2114-2123.